Int J Adv Manuf Technol (2018) 95:1205–1213
https://doi.org/10.1007/s00170-017-1276-z

ORIGINAL ARTICLE

# Precision forming of the 3D curved structure parts in flexible multi-points 3D stretch-bending process

**Song Gao[1] · Ji-cai Liang[2] · Yi Li[2] · Zhao-peng Hao[1] · Qi-han Li[1] · Yi-hang Fan[1] · Ying-li Sun[1]**

Received: 27 June 2017 / Accepted: 26 October 2017 / Published online: 8 November 2017


**Abstract** The lightweight aluminum 3D curved structure part has the characteristics of high structural strength, excellent aerodynamic performance, and flowing geometric shape. It is increasingly used in the fields of railway transportation, aerospace, and other high-end vehicle manufacture industry. However, with the increase of forming dimensions, as well as the large, thin-walled, complex forming features, it is urgent to study the precise plastic forming method for this kind of difficult-to-deform materials. Based on the new type of flexible multi-points 3D stretch-bending (3D FSB) process, the precision forming method for these hard-to-deform parts was studied in this paper. Extensive numerical simulations for the 3D FSB forming of the target parts have been performed by finite element methods. The simulation results show good agreement with the experiment results, and the max shape error of springback prediction is less than 0.3 mm. Then, based on the measured shape error of the 3D formed parts, an iterative overbending method for envelope surface of the multi-point die (MPD) is proposed to realize precise forming of the 3D curved structure parts. After four times adjustment of MPD, the simulation results show that the contour error is reduced from 1.01 to 0.06%, the maximum springback error changes from 30.16 to 1.66 mm. According to the adjustment parameters acquired in the optimization process, the actual experimental measured contour error is 0.05%, the maximum springback error is 1.41 mm, which achieved the forming requirements of the target parts and verified the effectiveness of the compensation method.

**Keywords** Multi-point forming · Flexible 3D stretch-bending · Springback compensation · Iterative overbending method · 3D curved structure part

## 1 Introduction

Since 3D curved aluminum structure component has the advantages of lightweight, high strength, and excellent aerodynamic performance, it is increasingly used in the fields of railway transportation, aerospace, and other high-end vehicle manufacture industry [1, 2]. As shown in Fig. 1, a typical 3D curved structure part was employed in the Chinese CRH380 series high-speed train's head skeleton. However, due to the characteristics of high deformation resistance, low plasticity, and narrow processing window of the material, as well as the large, thin-walled, and complex forming features of the target part, it is hard to precisely forming this kind of spatial components [3–5]. Therefore, the study of the accurate plastic forming method for this type of high-performance, lightweight components has been a hot topic and frontier in the field of metal material processing.

With the increase of the forming dimensions, the conventional bending process has been unable to satisfy the complex forming requirements at present. There are some new flexible multi-DOF bending technologies be developed in recent years. Based on the kinematic forming method, Chatti and Hermes developed the torque superposed spatial (TSS) bending process [1]. By using the three pairs of rolls and a roll-based guiding system (bending head), this method allows the bending of profiles with arbitrary cross-sections to arbitrary 3D curved contours. Besides, Muller developed a hot bending

✉ Ji-cai Liang
ltazh@qq.com

[1] School of Mechatronic Engineering, Changchun University of Technology, Changchun, Jilin province 130012, China

[2] College of Material Science and Engineering, Jilin University, Changchun, Jilin province 130022, China

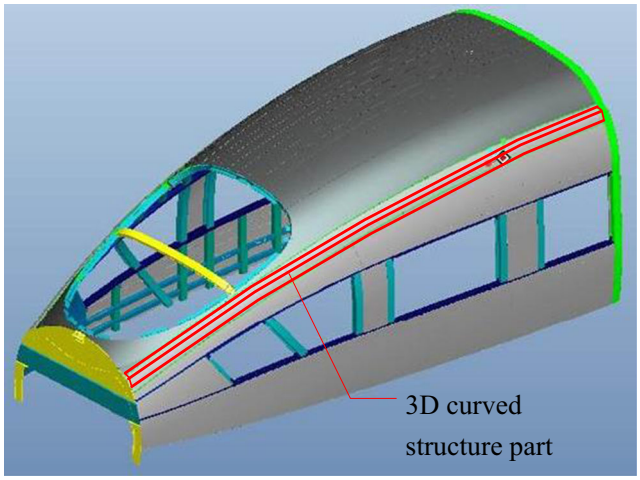


**Fig. 1** The skeleton of CRH380 series high-speed train

process [6], which directly bending the aluminum profiles during the extrusion process. Then, a new tool set up combines the extrusion-bending-quenching was designed by Li [7]. Another flexible bending process is the section bending technology which was proposed by Geiger [8]. It uses a roller-shaped upper punch, and a rubber pad as the lower die. The shape of the final part is depending on the indentation depth of the roller. Based on this forming principle, a forming prototype was developed by He [9]. In summary, these forming processes realize the complicated 3D bending of the profile; however, owing to the kinematic forming feature, they are not suitable for the batch production in the high-speed train's manufacturer because of the large, complex geometry features of the target parts.

In the face of high-speed train manufacturer demand, a new type of flexible multi-points 3D stretch-bending (3D FSB) process was proposed and implemented by Liang and Gao [10–13]. The 3D FSB process overcomes the shortcomings of low flexibility and only one direction bending feature in the traditional stretch-bending process. It achieves a fast, efficient, and flexible forming technology for 3D curved parts. However, due to the action of multi-axial forces and inhomogeneous deformation characteristics, the springback deformation seriously affects the accuracy of forming parts. Therefore, this paper first introduces the basic principle of 3D FSB process. Then, an iterative modification method for compensating the springback is proposed by using an overbending envelope surface. Extensive numerical simulations for the 3D FSB forming of the target parts have been performed by finite element methods. The experiments were conducted to verify the effectiveness of the proposed springback compensation method. The configuration of the deformed part was compared with the required objective shape. In conclusion, the modified envelope surface of MPD obtained from the iterative optimization method considerably improved the forming accuracy. The precise forming parts have been applied in the manufacture of Chinese CRH380 series high-speed trains.

## 2 Flexible multi-points 3D stretch-bending process

Multi-points forming (MPF) technology has been widely used in the field of sheet metal forming in recent years [14–18]. Based on MPF idea, the solid curved die in the traditional 2D stretch-bending process was separated into the multi-point dies (MPD) in the 3D FSB process. The reconfigurable die surfaces of this new process make it is possible to realize 3D curved parts' forming. As shown in Fig. 2, the forming principle of the 3D FSB process can be described as followed: First, the envelope surface of a set of MPD which installed on the flexible fundamental units (FFU) was adjusted to the shape of the target part. Under a constant axial force loaded by the two tensile hydraulic actuators, the workpiece is stretched into the plastic state. Then, the workpiece will gradually contact with the MPD from the center to the two sides by the horizontal moment. Once the workpiece fully contacted with the MPD, the vertical hydraulic loads are applied to form the workpiece in the vertical direction. With the clamps turn to the setting positions, a 3D curved part was successfully formed in this process. There will be a post-stretch process

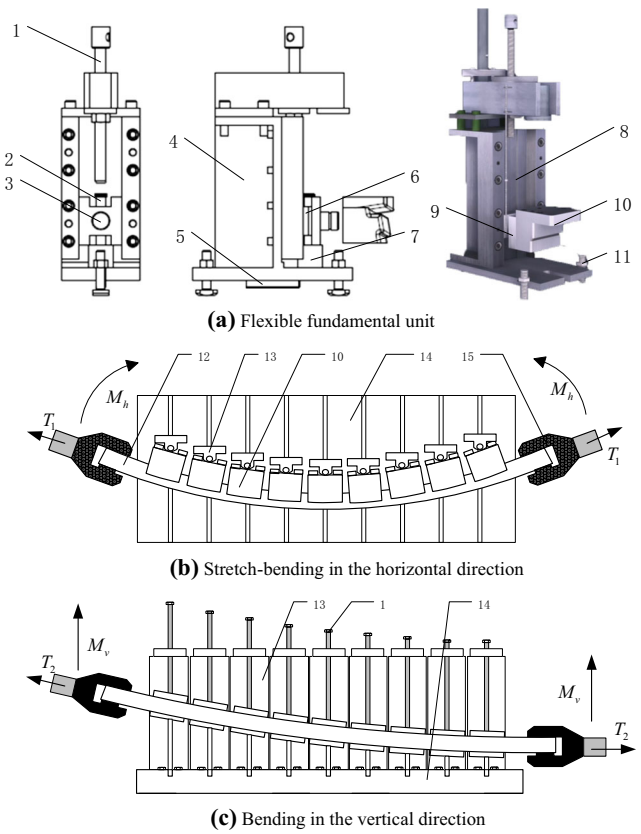


**Fig. 2** Schematic diagram of 3D FSB

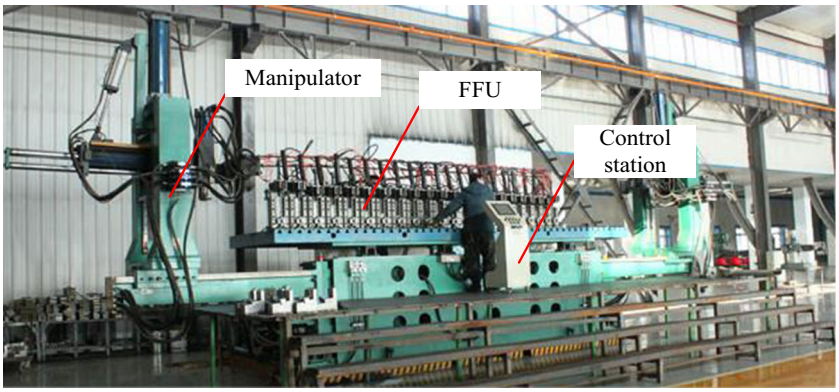


**Fig. 3** The prototype of FSB equipment

at last to reduce the effect of springback. Different shapes of 3D parts can be formed by adjusting the position of MPD in the horizontal direction and vertical direction.

The structure of FFU is shown in Fig. 2a. As the carrier of the MPD, the FFU realizes the 4-DOF of MPD which is both the movement and rotation in the horizontal and vertical directions to deform the 3D curved parts. The structure of the FFU has the following properties. (1) Reconfigurable die surface, which increased flexibility of the stretch-bending process; (2) Local position adjustable, the springback can be effectively controlled; and (3) Fast changeable MPD, the MPD can be quickly changed if the cross-section shape and type are different.

This new forming process solves the problems of high cost, poor flexibility and cannot 3D bend in the conventional 2D stretch-bending process. It is very suitable to manufacture that kind of thin-walled complex shape 3D components in the high-speed trains. Based on the 3D FSB forming principle, the prototype of FSB equipment was developed, which is shown in Fig. 3.

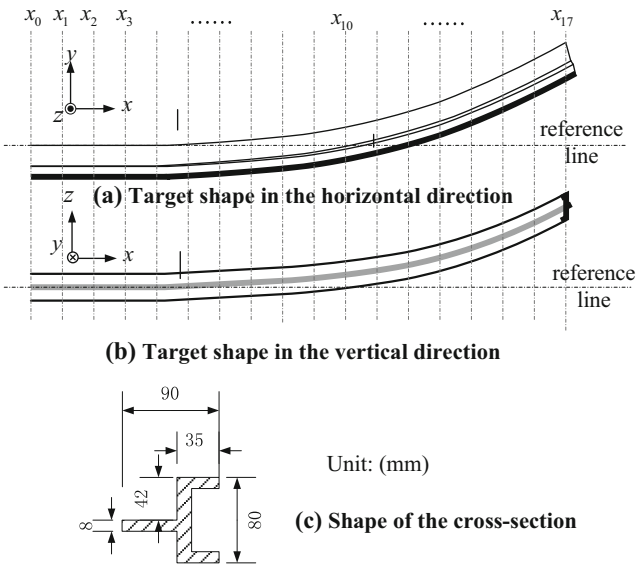


**Fig. 4** Target geometry shape of the structural part for the high-speed trains

## 3 Numerical simulation of 3D FSB process

### 3.1 Forming requirement of the target part

As the key frame structure of the skeleton in the high-speed trains, the target geometry and cross-section shape of the 3D curved structure part are shown in Fig. 4.

As shown in Fig. 4, the target shape of 3D curved structure part has the features of asymmetric geometry and different curvature in the horizontal and vertical directions. The length of the aluminum workpiece is 4.5 m, and the cross-section of the workpiece is irregular T profile, its web is located inside during the forming process. In order to realize the accurate assembly of this part, the forming contour error should be controlled within 0.1%; the maximum springback error is required less than 2 mm, which proposes a strict requirement on the forming process. As shown in Fig. 5, the fitting characteristic curves of the target part were defined by the discrete control vertex. The points in Fig. 5 indicate the coordinates of the MPD in the *y*-axis and the *z*-axis, which is according to the position of each MPD in *x*-axis direction. The adjustment parameters of each MPD can be calculated

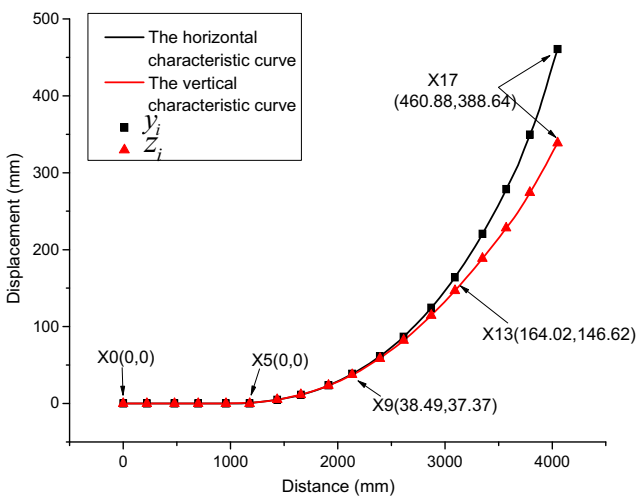


**Fig. 5** The characteristic curves of the structural part for high-speed trains

**Table 1** Mechanical properties of the material

| Parameters | Value |
|---|---|
| Elastic modulus $E$(Gpa) | 65.05 |
| Yield strength $\sigma_s$(Mpa) | 188.44 |
| Poisson's ratio $\upsilon$ | 0.3 |
| Strength factor $K$(Mpa) | 452.64 |
| Strain-hardening $n$ | 0.15 |

according to the characteristic curves of the target part, which is specific in reference [11].

### 3.2 Material model

The materials of the aluminum profile used for this part are aluminum alloy T6065, which is extensively applied in high-speed trains' structural parts. The material parameters of the aluminum profile are shown in Table 1. In the material model, the workpiece is assumed that the materials obeyed the Von Mises yield criterion and Prandtl-Ruess flow rule. And the material is performed isotropic both in the strain-hardening model and the elastoplastic constitutive behavior. For small elastic deformation, the stress satisfies Hooke's law. For large deformation, the stress is proportional to the strain to the power of $n$, which is the strain-hardening exponent. Therefore, the relationship between stress and strain can be express as:

$$\begin{aligned} \sigma &= E\varepsilon \quad for \quad \sigma < \sigma_s \\ \sigma &= K\,\varepsilon^n \quad for \quad \sigma \geq \sigma_s \\ \sigma &= -K|\varepsilon|^n \quad for \quad \sigma \leq -\sigma_s \end{aligned} \tag{1}$$

where $K$ is the strength coefficient, the value is shown in Table 1.

### 3.3 FE model of simulation

Commercial finite element software ABAQUS/explicit is chosen to conduct numerical simulations for FSB process due to the advantages in solving nonlinear problems. Besides, the forming process is a large deformation and dynamic process, so it is suitable using explicit procedure over the implicit

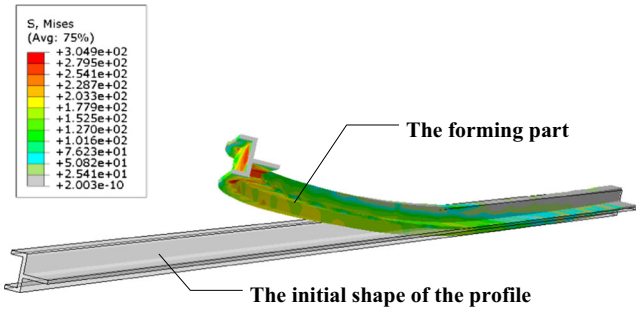


**Fig. 7** The CAE simulation results of high-speed trains' structural part

procedure in complicated contact conditions [19–21]. Based on the characteristic curves of the target part in the 3D FSB process, the finite element simulation model of the forming process was established, as shown in Fig. 6.

The aluminum profile is dispersed into many C3D8R solid elements. The model is mainly composed of the deformable T profile workpiece and the rigid MPD in 1:1 scale. There are 18 MPD used in the forming process. The envelope surface of MPD was adjusted according to the shape of the target part. The forming process is divided into four steps, which are the pre-stretch, the horizontal bending, the vertical bending, and the post-stretch process. The forming process is controlled by displacement loading of the clamp, which is abstracted as a hinge point with six degrees of freedom. The clamp connected with the profile by establishing the joint rigid-connecting elements. The contact between profile and MPD is defined as the surface contact. The friction coefficient is set up to be 0.1 in the simulation. The horizontal envelope shape of the MPD was adjusted before simulation. The vertical shape was controlled by the translation connector elements established on each MPD. The simulation results of the forming process are shown in Fig. 7. It can be seen that the workpiece was formed both in the horizontal and vertical directions. The stress distribution along the axial direction of the workpiece is uniform, and the maximum stress occurred at the clamping position of the formed part.

Since the springback is the main factor affecting the accuracy of forming parts, it is essential to predict the springback in

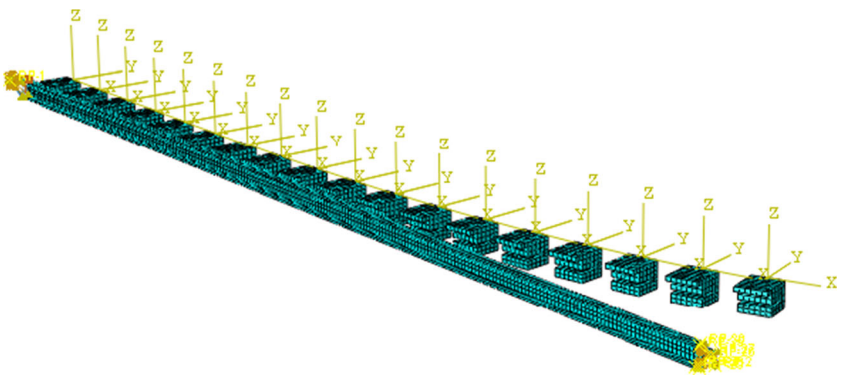

**Fig. 6** The CAE simulation model of high-speed trains' structural part

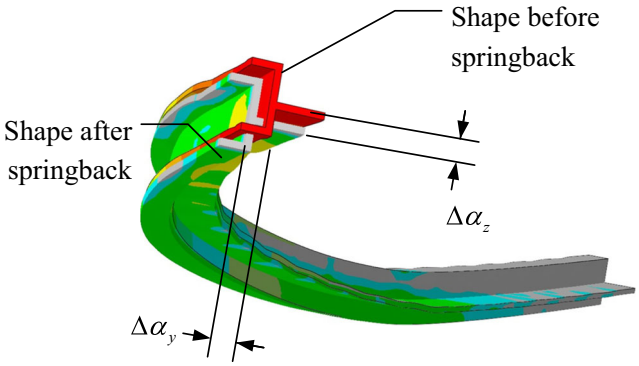


**Fig. 8** The shape change after springback

the numerical simulation [22, 23]. By using the function of the predefined field in Abaqus, based on the state of stress and strain distribution results, the springback prediction model was established. The springback process is moving from one equilibrium to another. Therefore, the implicit procedure was taken to provide better results in this analysis. In order to observe the springback phenomenon caused by the forming outputs, the loads, and the boundary conditions were deleted in springback simulation. Figure 8 demonstrates the shape changes of the formed part before and after springback. Because of the springback effect, the maximum shape deviation reached 30 mm. The formed part could not meet the requirement of forming accuracy.

## 4 Precision forming of 3D curved parts for high-speed trains

Based on the flexible envelope surface feature of the FSB process, the general procedure from the design of the object shape to the precision manufacture of the product is shown in Fig. 9. In this study, the FE model was used in optimizing the envelope surface of MPD. According to the simulation results, the shape error is examined by the following evaluation method for FSB process. If the forming accuracy does not meet the requirements, the die surface will be regenerated by the springback compensation method until the target shape is obtained. The forming experiments will be carried out to test whether the actual forming accuracy reaches the forming requirements.

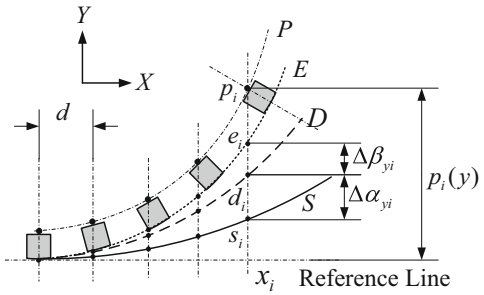


**(a)** The Horizontal direction

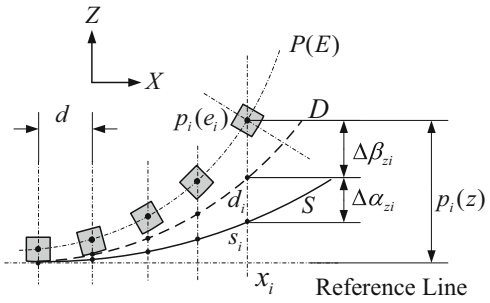


**(b)** The Vertical direction

**Fig. 10** Definition of springback in FSB process

### 4.1 Evaluation method of the formed parts in 3D FSB process

In order to research the relationship between springback and the adjustment parameters of MPD, the evaluation method of forming accuracy for the 3D stretch-bending parts is proposed as shown in Fig. 10. In this figure, $P$ is the fitting characteristic curve of the MPDs' adjustment parameters; $E$ is the curve of envelope surface of MPD; $D$ is the characteristic curve of the target part; and $S$ is the final shape of the forming part after springback. In the horizontal direction, $P$ and $E$ are equidistant curves, while in the vertical direction they are coincident. The $p_i$, $e_i$, $d_i$, and $s_i$ are the coordinates according to the MPD's position on the $x$-axis. The subscript $i(i = 0, 1, 2, 3 .. \ldots N)$ represents the number of each MPD. $\Delta\alpha$ is the measured springback error on the cross-section which is defined in Fig. 8. $\Delta\beta$ is the compensation displacement of MPD. Mathematically, these variables defined above have the following relationships:

$$\Delta\alpha_i = s_i - d_i \tag{2}$$

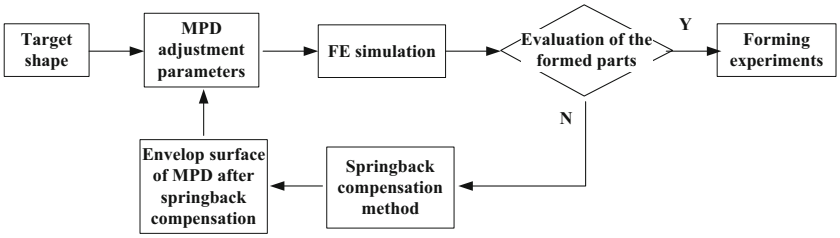


**Fig. 9** The procedure of precision forming for the FSB process


**Fig. 11** The springback detector for FSB process

$$e_i = d_i - \Delta\beta_i \tag{3}$$

The local springback ratio and the contour error of the formed part are defined as:

$$\delta_i = \frac{\Delta\alpha_i}{d_i} \tag{4}$$

$$\Delta\phi = \frac{1}{N+1}\sqrt{\sum_{i=0}^{N}\left(\frac{(\Delta\alpha_{yi})^2 + (\Delta\alpha_{zi})^2}{(d_i(y))^2 + (d_i(z))^2}\right)} \tag{5}$$

Where $\Delta\alpha_{yi}$ and $\Delta\alpha_{zi}$ are the horizontal and vertical shape error at the $i$th MPD; $d_i(y)$ and $d_i(z)$ are the horizontal and vertical coordinates of the target shape corresponding to the $i$th MPD's $x$-axis position. The contour error $\Delta\phi$ considers the relative shape error of each adjustment point, and it can describe the overall forming accuracy of the 3D stretch-bending part.

The advantages of this 3D springback evaluation method are the following: (1) It clarifies the relation between springback and profile adjustment parameters; (2) The law of springback variation along the profiles can be researched; and (3) The basis of error compensation for each MPD is given in the measurement. Based on this evaluation method, the springback detector for FSB process was developed as shown in Fig. 11. According to the MPDs' $x$-axis adjustment parameters, the springback detector is regularly arranged as the target part's shape. The shape errors of the 3D stretch-bending part in $y$-axis and $z$-axis after springback can be easily examined and measured in the actual experiments.

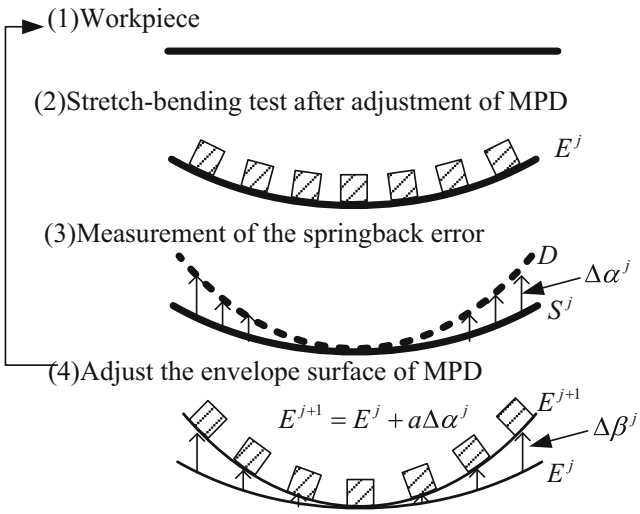


**Fig. 12** The displacement adjustment method for FSB process

### 4.2 Springback compensation method

In order to overcome the effect of springback on forming accuracy, several compensation methods were proposed by using numerical approaches. Among these methods, the displacement adjustment method (DA method) and the spring-forward method are widely used in sheet metal forming process. The DA method using the displacement of shape error inversely imposed on the target surface to make a new die shape [24, 25]. The spring-forward method using the formed stresses inversely imposed on the target part to get the overbending die surface [26]. Compared with the spring-forward method, the DA method has the advantage of less iterations and it does not have the iteration non-convergence problem. Therefore, based on the DA method, the iterative overbending method for FSB process is proposed, which is shown in Fig. 12. The initialize adjustment is using the target shape as the envelope surface of MPD. The superscript $j$ is the number of iteration.

$$E^1 = D \tag{6}$$

The envelope surface of MPD after iterative compensation is:

$$\begin{aligned} E^{j+1} &= E^j + a\cdot\left(S^j - D\right) \\ e_i^{j+1} &= e_i^j + a\left(s_i^j - d_i\right), (i = 0, 1, 2, 3, \ldots\ldots, N) \end{aligned} \tag{7}$$

$a$ is the springback compensation factor, which can help to accelerate the iterative process, generally its value from − 2.5 to − 1.

As the springback error of the formed part meets the following criteria:

$$\left\|S^j - D\right\|_{\max} < \lambda_1, \&(\Delta\phi < \lambda_2) \tag{8}$$

The iterative process will stop. In these formulas, $\Delta\phi$ defined in Eq. 5 is the contour error, $\lambda$ is the requirement of forming precision. Besides, $\Delta\alpha^j$ and $\Delta\beta^j$ in Eqs. 2 and 3 can be expressed as:

$$\Delta\alpha_i{}^j = S_i^j - D_i \tag{9}$$

$$\Delta\beta_i^j = a\Delta\alpha_i^j \tag{10}$$

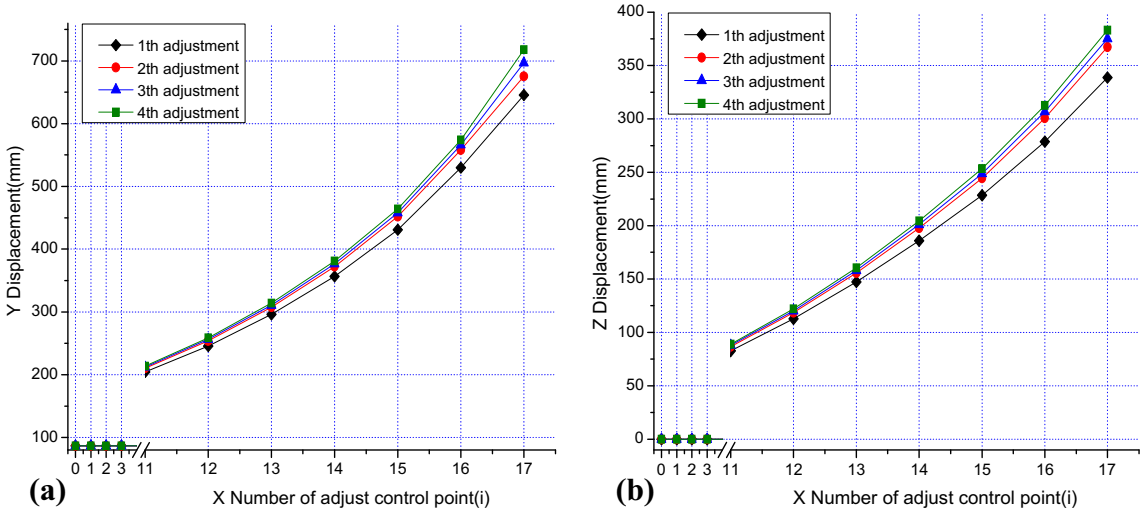


**Fig. 13** The adjustment characteristic curves of MPD in the horizontal and vertical directions. **a** The horizontal adjusting curves. **b** The vertical adjusting curves

At last, the adjustment parameters of each MPD will be calculated by the compensation data of envelope shape as follows:

$$\begin{aligned} P_y^{j+1} &= E_y^{j+1} \pm \overrightarrow{n}_{E_y^{j+1}} R_h \\ P_z^{j+1} &= E_z^{j+1} \end{aligned} \tag{11}$$

Where $\overrightarrow{n}_{E_y^{j+1}}$ is the normal vector of the horizontal adjustment curve $P_y$, and $R_h$ is the rotation radius of MPD which is a constant.

### 4.3 Application of springback compensation method

According to the forming requirements of the 3D curved part for high-speed trains, the overall contour error $\Delta\phi$ should be less than $\lambda_2 = 0.1\%$, and the maximum springback error should be less than $\lambda_1 = 2$ mm. Based on the DA method and the established simulation model, the 3D stretch-bending part satisfying the forming accuracy was realized after 4 times adjustment. In these 4 times simulation, the characteristic curves of the MPD's adjustment control points are shown in Fig. 13. The overall contour error changes from 1.01% at the first adjustment to 0.06% at the fourth adjustment. The maximum springback error changes from 30.16 to 1.66 mm.

The springback ratio $\delta$ in Eq. 4 is defined as the ratio of the measured shape error and the target coordinates at each position of MPD, its change in these four times adjustment are demonstrated in Fig. 14.

At the first adjustment, by using the target shape as the envelope surface of MPD, the formed part has a large springback

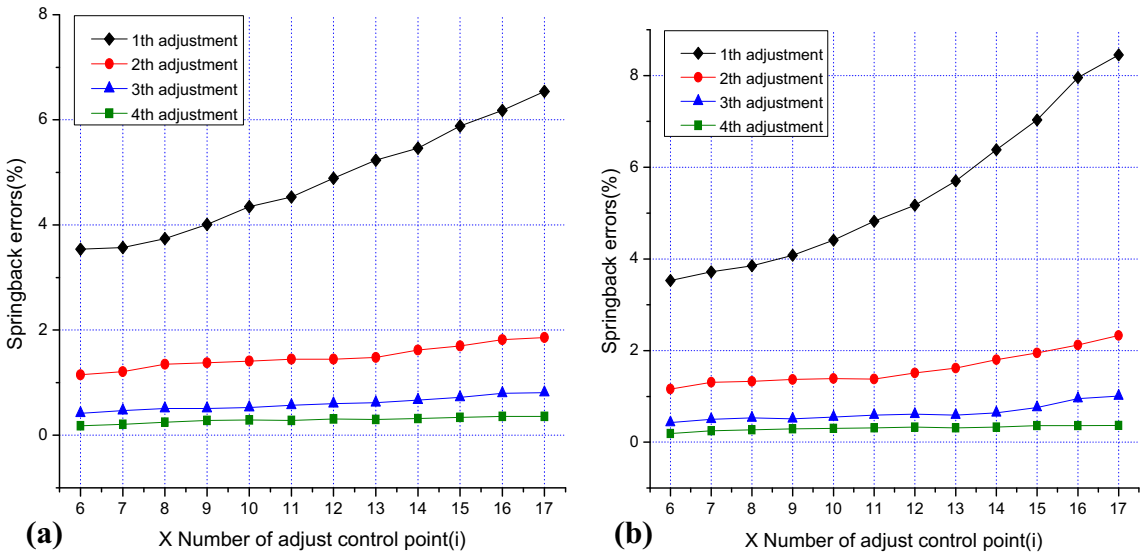


**Fig. 14** The changes of springback ratio. **a** The horizontal springback ratio. **b** The vertical springback ratio

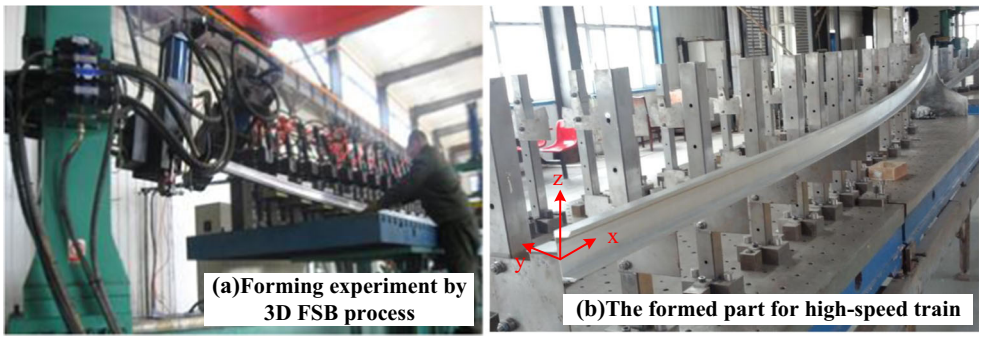


**Fig. 15** The forming experiment of 3D FSB process

ratio. The maximum springback ratio is 6.54% in the horizontal direction, and 8.45% in the vertical direction. With the increase of deformation displacement, the springback ratio also increases. At the second adjustment, the change of the springback ratio flattens out gradually. The maximum springback ratio reduced to 1.86% in the horizontal direction, and 2.33% in the vertical direction. After four times adjustment, these data changed to 0.35 and 0.37%. The simulation results show that the DA method for the envelope surface compensation can improve the shape deviation effectively. The required forming precision can be achieved by using iterative optimization method in CAE simulation.

## 5 Forming experiments

Based on the adjustment parameters acquired in the optimization process, the actual forming experiment was carried out to confirm the forming accuracy of the modified die shape by the 3D FSB equipment, which is shown in Fig. 15a. The formed 3D curved structure part for the high-speed trains is shown in Fig. 15b, which is placed on the springback detector. The experimental shape error can be measured on the springback detector, which is regularly arranged according to the adjustment parameters of each MPD. The results of experiments and FE simulation are compared as shown in Fig. 16. It can be seen that the FE simulation predicts the trend of springback efficiently; the max absolute error between simulation and experiment is less than 0.3 mm. Experiment results verify the accuracy of the FE simulation.

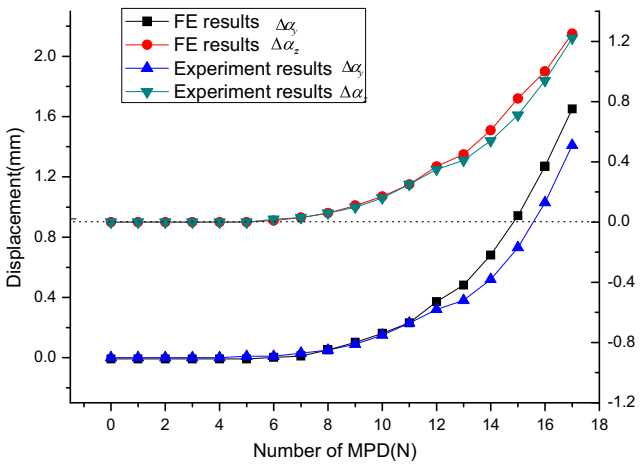


**Fig. 16** The comparison between experiment and FE simulation results

The max springback values representing the forming precision are demonstrated in Table 2. According to the experimental results of springback measurement, the overall contour error $\Delta\phi$ is 0.05% calculated by Eq. 5, which is required less than 0.1%. The maximum measurement springback error is 1.41 mm, which is required less than 2 mm. Thus, the precision forming of the 3D curved structure part for the high-speed train is realized by the 3D FSB process.

## 6 Conclusions

The 3D curved structure parts assembling in the high-speed trains proposed a strict forming requirement for the forming process. Based on the new type of 3D FSB process, the precision forming method for these hard-to-deform parts was studied in this paper. Extensive numerical simulations for the 3D FSB forming of the target parts have been performed by finite element methods. The experimental results show good agreement with the FE simulation. This research will provide valuable and sufficient guidance on determining the 3D FSB parameters and optimizing the 3D FSB process.

According to the forming demand of the 3D curved structure part for high-speed trains, a numerical simulation model has been established to analysis the forming process and springback phenomenon by the dynamic explicit and static implicit procedure. Numerical results of springback prediction on the target part are in good agreement with the experimental results, and the max absolute error is less than 0.3 mm.

**Table 2** The experiment results of 3D stretch-bending

| Item | FE simulation | Experiments | Error (%) |
|---|---|---|---|
| Max $\Delta\alpha_y$(mm) | 1.66 | 1.41 | 17.7 |
| Max $\Delta\alpha_z$(mm) | 1.25 | 1.22 | 2.45 |
| $\Delta\phi$ (%) | 0.06% | 0.05% | |

Based on the forming accuracy evaluation method for the formed parts, an iterative optimization method for the envelope surface of MPD is proposed by displacement adjustment. The simulation results show that the contour error is reduced from 1.01 to 0.06%. The maximum springback error changes from 30.16 to 1.66 mm after four times adjustment. The springback can be reduced significantly by the proposed method.

The 3D stretch-bending experiments using the 3D FSB apparatus were carried out to verify the feasibility of the springback compensation approach. It was also noted that the modified envelope shape of MPD obtained from the iterative optimization method considerably improved the forming accuracy. The experimental measured contour error is 0.05%, and the maximum springback error is 1.41 mm. They are less than the 0.1% and 2 mm forming requirements. Accurate forming of the target part is achieved in 3D FSB process. At present, the precise forming parts have been used in the manufacture of Chinese CRH380 series high-speed trains. The 3D FSB process and equipment have implemented industrialized production.

**Funding Information** The National Natural Science Foundation of China (51675225) provided the financial support.

## References

1. Chatti S, Hermes M, Tekkaya AE, Kleiner M (2010) The new TSS bending process: 3D bending of profiles with arbitrary cross-sections. CIRP Ann Manuf Technol 59(1):315–318
2. Hermes M, Staupendahl D, Becker C, Tekkaya AE (2011) Innovative machine concepts for 3D bending of tubes and profiles. Key Eng Mater 473:37–42
3. Zhan M, Wang Y, Yang H, Long H (2016) An analytic model for tube bending springback considering different parameter variations of Ti-alloy tubes. J Mater Process Technol 236:123–137
4. Dong J, Liu Y, Yang H (2016) Research on the sensitivity of material parameters to cross-sectional deformation of thin-walled rectangular tube in rotary draw bending process. J Mater Res 31(12): 1784–1792
5. Liu N, Yang H, Li H, Yan S (2016) Plastic wrinkling prediction in thin-walled part forming process: a review. Chin J Aeronaut 29(1): 1–14
6. Müller KB (2006) Bending of extruded profiles during extrusion process. Int J Mach Tool Manu 46(11):1238–1242
7. Luoxing LI (2012) Advanced extrusion technology and application of aluminium, magnesium alloy for vehicle body. J Mech Eng 48(18):35 **(in Chinese)**
8. Geiger M, Arnet H, Vollertsen F (1995) Flexibles Biegen Stranggepresster Aluminium profile. Blech Rohre Profile 42(1): 31–34
9. Zhu-Bin HE, Lin YL, Sun HY (2012) On curvature radius of profiles bent with single roller and hyper-elastic pad. Mater Sci Technol 20(5):1–5
10. Liang JC, Gao S, Teng F, Yu PZ, Song XJ (2014) Flexible 3D stretch-bending technology for aluminum profile. Int J Adv Manuf Technol 71(9–12):1939–1947
11. Gao S, Liang JC, Teng F, Chen GY, Wei ZY (2014) Shape control of parts formed by means of flexible 3D stretch-bending technology. Huanan Ligong Daxue Xuebao/J South China Univ Technol 42(9):53–58 **(in Chinese)**
12. Gao S, Liang JC, Chen GY, Wei ZY, Teng F (2014) Rapid adjusting of fundamental units in process of flexible 3D stretch-bending. Jilin Daxue Xuebao 44(6):1723–1727 **(in Chinese)**
13. Teng F, Zhang W, Liang J, Gao S (2015) Springback prediction and optimization of variable stretch force trajectory in three-dimensional stretch bending process. Chin J Mech Eng 28(6): 1132–1140
14. Cai ZY, Wang SH, Xu XD, Li MZ (2009) Numerical simulation for the multi-point stretch forming process of sheet metal. J Mater Process Technol 209(1):396–407
15. Amini M, Bakhshi M, Fesharaki JJ (2014) Design, fabrication, and use of a new reconfigurable discrete die for forming tubular parts. Int J Adv Manuf Technol 75(5–8):1055–1063
16. Wang S, Cai Z, Li M, Lan Y (2012) Numerical simulation on the local stress and local deformation in multi-point stretch forming process. Int J Adv Manuf Technol 60(9–12):901–911
17. Heo SC, Kim JN, Song WJ, Ku TW, Kang BS (2012) Shape error compensation in flexible forming process using overbending surface method. Int J Adv Manuf Technol 59(9–12):915–928
18. Abosaf M, Essa K, Alghawail A, Tolipov A, Su S, Pham D (2017) Optimisation of multi-point forming process parameters. Int J Adv Manuf Technol 92(6):1–11
19. Cai ZY, Wang SH, Li MZ (2008) Numerical investigation of multi-point forming process for sheet metal: wrinkling, dimpling and springback. Int J Adv Manuf Technol 37(9–10):927–936
20. Wang S, Cai Z, Li M (2010) Numerical investigation of the influence of punch element in multi-point stretch forming process. Int J Adv Manuf Technol 49(5–8):475–483
21. Li L, Seo YH, Heo SC, Kang BS, Kim J (2010) Numerical simulations on reducing the unloading springback with multi-step multi-point forming technology. Int J Adv Manuf Technol 48(1–4):45–61
22. Wagoner RH, Lim H, Lee M-G (2013) Advanced issues in springback. Int J Plast 45(0):3–20
23. Tan F, Li M, Cai Z, Li X (2009) Formability analysis on the process of multi-point forming for titanium alloy retiary sheet. Int J Adv Manuf Technol 41(11–12):1059–1065
24. Lingbeek RA, Gan W, Wagoner RH, Meinders T, Weiher J (2008) Theoretical verification of the displacement adjustment and springforward algorithms for springback compensation. Int J Mater Form 1(3):159–168
25. Yang XA, Feng R (2011) A die design method for springback compensation based on displacement adjustment. Int J Mech Sci 53(5):399–406
26. Karafillis AP, Boyce MC (1992) Tooling design accomodating springback errors. J Mater Process Technol 32(1–2):499–508